J Neurophysiol 130: 168–178, 2023.
First published June 21, 2021; doi:10.1152/jn.00518.2022

american physiological society

JNP JOURNAL OF NEUROPHYSIOLOGY

RESEARCH ARTICLE

Society for the Neural Control of Movement

Comparison of vestibular input statistics during natural activities and while piloting an aircraft

Axel Roques,[1,2,3] Yannick James,[3] Ioannis Bargiotas,[1] Dimitri Keriven Serpollet,[1] Nicolas Vayatis,[1] and Pierre-Paul Vidal[1,4,5]

[1]*Centre Borelli, CNRS, SSA, INSERM, Université Paris Saclay, ENS Paris Saclay, Université Paris Cité, Paris, France;* [2]*Laboratoire GBCM, EA7528, CNAM, Hesam Université, Paris, France;* [3]*Thales AVS, Osny, France;* [4]*Institute of Information and Control, Hangzhou Dianzi University, Hangzhou, China; and* [5]*Plateforme d'Etude Sensorimotricité, CNRS UAR2009, INSERM US36, Université Paris Cité, Paris, France*

Abstract

The present study investigates the statistics and spectral content of natural vestibular stimuli experienced by healthy human subjects during three unconstrained activities. More specifically, we assessed how the characteristics of vestibular inputs are altered during the operation of a complex human-machine interface (a flight in a helicopter simulator) compared with more ecological tasks, namely a walk in an office space and a seated visual exploration task. As previously reported, we found that the power spectra of vestibular stimuli experienced during self-navigation could be modeled by two power laws but noted a potential effect of task intensity on the transition frequency between the two fits. In contrast, both tasks that required a seated position had power spectra that were better described by an inverted U shape in all planes of motion. Taken together, our results suggest that *1*) walking elicits stereotyped vestibular inputs whose power spectra can be modeled by two power laws that intersect at a task intensity-dependent frequency; *2*) body posture induces changes in the frequency content of vestibular information; *3*) pilots tend to operate their aircraft in a way that does not generate highly nonecological vestibular stimuli; and *4*) nevertheless, human-machine interfaces used as a means of manual navigation still impose some unnatural, contextual constraints on their operators.

NEW & NOTEWORTHY Building upon previously published research, this study assesses and compares the vestibular stimuli experienced by healthy subjects in natural tasks and during the interaction with a complex machine: a helicopter simulator. Our results suggest the existence of an anatomical filter, meaning that body posture shapes vestibular spectral content. Our findings further indicate that operators control their machine within a constrained operating range such that they experience vestibular stimulations that are as ecological as possible.

head movements; human-machine interaction; natural tasks; vestibular information

INTRODUCTION

Adequate processing of vestibular stimuli is instrumental in selecting the appropriate strategy for movement control. In that context, a number of recent studies have characterized the properties of active and passive head movements experienced during daily activities (1–3). Contrary to self-generated active head movements, passive head movements occur during external postural perturbations. Carriot et al. (1) found that active head movements reached magnitudes of 450°/s, with long-tailed non-Gaussian probability density functions when projected on the three planes of the semicircular canals: the left anterior, right posterior (LARP) plane, the right anterior, left posterior (RALP) plane, and the yaw plane (YAW). During natural activities, the power spectrum of both active and passive head movements could be fitted with two power laws. The first power law models the slow decrease observed for the low frequencies (<5 Hz in Ref. 1 or <2 Hz in Ref. 2), and the second models the steeper decrease for higher frequencies. This result differs from the other sensory modalities, where a single power law is often observed (4): both biomechanical preneuronal filtering and voluntary

Correspondence: P.-P. Vidal (ppvidal@me.com).
Submitted 28 December 2022 / Revised 11 May 2023 / Accepted 7 June 2023

control shape the spectral content of natural vestibular inputs (1).

These studies focused on a large set of natural activities (see Ref. 1 for a complete list). In contrast, the properties of head movements experienced during the control of complex human-machine interfaces remain largely unknown. To investigate this matter, we asked whether the vestibular inputs experienced by the operators of a human-machine interface would present the same statistics as during more ecological activities. The answer to this question appears valuable on two grounds. First, a substantial part of human activities relies on the use of complex human-machine interfaces. Second, individuals should be considered as *embodied*, i.e., as part of a system that involves their immediate environment (5, 6). That is, when interacting with a machine, one is submitted to sensory afferences that may be sensibly different from those experienced during ecological tasks. For instance, externally imposed motion was found to challenge both perception and motor control; in particular the frequency range 0.2–0.3 Hz constitutes the possible origin of the "tilt-translation" ambiguity and could induce motion sickness (7). In turn, such uncommon inputs could deeply alter the perceptual and behavioral responses of the operators and may have detrimental practical consequences (increased mental load, false maneuvers, etc.).

We chose to explore the natural repertoire of head movements of helicopter pilots during flights in a simulator. Indeed, helicopter pilots constitute the archetypal operator of a complex human-machine interface. Moreover, the sensory systems of pilots are solicited in two complementary ways: *1*) during self-generated motions of the head (e.g., during the visual exploration of the outside world and of the cockpit) and *2*) during the unusual stimuli caused by the movements of the aircraft, whether initiated voluntarily or provoked by turbulences. In both cases, the sensory afferences experienced by the pilots are, at least partly, shaped by the peculiar dynamics of the aircraft and the flying environment. Therefore, they may be very different from those generated during day-to-day activities and more complex to match the expected sensorial reafferences required for an efficient motor control (8).

To compare the properties of vestibular stimuli experienced during an interaction with a machine to those experienced during more ecological activities, the head movements of healthy human subjects were measured in three experiments: a helicopter flight simulation (which we refer to as the manual navigation task), a walk in an office space (the self-navigation task), and a seated head-free visual exploration task (the seated visual exploration task). Our findings complete and extend recent work on the statistics of vestibular inputs during daily life activities. In all planes of motion, the power spectra of vestibular stimuli during self-navigation were well fitted with the previously proposed model (1), albeit we found a possible effect of task intensity on the transition frequency. We further demonstrate that the frequency content of natural vestibular stimuli differs according to body posture, suggesting the presence of an *anatomical filter*. In the manual navigation task, pilots experienced rather unecological vestibular stimulation compared with other tasks, yet the characteristics of their head movements remained roughly comparable to the seated visual exploration task, which presumably indicates that they control their machine in such a way as not to experience vestibular stimuli that are too far apart from what they experience on a daily basis. We discuss the implications of manual navigation tasks for the study of the selective processing of passively experienced vestibular inputs.

MATERIALS AND METHODS

The Institutional Review Board Paris Descartes (CERES No. 2017-35 dated 23-5-2017) approved the experimental flight protocols, following the 1964 Declaration of Helsinki. Before testing, all participants gave their written informed consent.

Manual Navigation Task

Nine operational helicopter pilots participated in the manual navigation task. Because of measurement issues, only seven pilots produced exploitable data, resulting in a final cohort of $N = 7$ males (39.6 ± 5.5 yr old). They had no known history of balance impairment or dizziness. Although all participants were professional pilots, their background and expertise level varied. A summary of pilot information can be found in Table 1.

The experiment was conducted in a full-flight level-D helicopter simulator (Fig. 1*A*). This simulator provided an accurate visual environment that covered the entire field of view and was supported by a six-degrees-of-freedom mobile platform driven by state-of-the-art algorithms (9, 10). It obtained the highest certification in terms of immersion and therefore truthfully reflects the vestibular stimuli experienced by pilots during real flights. The simulator was equipped with an EC135 (Eurocopter) helicopter cabin. Before the experiment, all pilots completed a realistic flight simulation to familiarize themselves with this specific simulator.

The manual navigation task consisted of two scenarios: the first was a reconnaissance mission, and the second was a rescue mission (Fig. 1*B*). A detailed description of the scenarios can be found in Supplemental Fig. S1 (all Supplemental Material is available at https://doi.org/10.5281/zenodo.8016675). Simulator motion was tightly linked to the trajectory taken by the pilots. Since piloting a helicopter is a task whose execution is extremely flexible, simulator motion was necessarily different from pilot to pilot. However, both missions consisted of typical subtasks that induced globally comparable movements of the simulator and thus similar head motion.

Head movements were measured at 100 Hz with an inertial-optical hybrid head tracker (IS-1200 + HObIT System, InterSense). This head-mounted sensor has the advantage of correcting for the inertial drift of traditional inertial measurement units (IMUs) by tracking the position of small fiducial markers on top of the cockpit with a camera, resulting in accurate measurements of head position in the reference frame of the simulator. Besides being easy to integrate in the pilots' equipment, the HObIT also proved to be robust when subjected to the nonnegligible external electromagnetic perturbations of the helicopter cabin. These two points were the impetus for the adoption of this sensor over a standard IMU. From the head position information, velocity signals were obtained by sample-to-sample numerical derivation. Complementary experiments that compared such velocity estimates with direct velocity

Table 1. *Summary of pilot information*

Pilot	Age, yr	Real Flight Experience, h	Last 12 Months, h	Simulator Experience, h	Background
1	41	2,100	190	26	Marine police, army
2	36	2,450	230	25	Army
3	47	1,840	200	28	Air force
4	34	300	120	30	Police
5	34	1,200	200	7	Air force (planes), police (helicopters)
6	37	965	120	90	Air force (planes and helicopters)
7	48	5,000	54	450	Air force (planes and helicopters)

Seven professional pilots participated in the manual navigation task. They had different backgrounds and different levels of expertise.

measurements from an IMU (XSens Dot, Movella) found similar values.

An eye tracking device (SMI Eye Tracking Glasses) was used to record the eye movements of pilots with a sampling frequency of 60 Hz, later upsampled at 100 Hz for sensor fusion purposes. A custom calibration step (6-point calibration) was conducted at the beginning and at the end of each experiment to ensure precise eye tracking during the whole experience. The direction of the eye movement during a simultaneous head rotation was used to distinguish between epochs of gaze redirection and gaze stabilization.

Self-Navigation Task

Eleven subjects (33.8 ± 13.5 yr old, 1 female) participated in the self-navigation task. They had no known history of balance impairment or dizziness. Because of limited pilot availability (see *Limitations*), these participants were distinct from those tested in the manual navigation task.

In this experiment, participants were asked to walk along a specific path for roughly 5 min in the corridors of an office space. The path consisted of going down and up a flight of stairs, 6 right turns, 6 left turns, and 2 U-turns. The experiment was conducted once for every participant.

Participants were equipped with an inertial measurement unit (XSens Dot, Movella) firmly fixed on their head with a head band. Head velocity was measured at 120 Hz and retrieved with the XSens Dot proprietary mobile application. In total, 52 min and 12 s of head velocity signals was captured.

Seated Visual Exploration Task

The same 11 subjects from the self-navigation task participated in the seated visual exploration task. In this experiment, participants were seated on a chair placed at the center of an office and were asked to explore their environment visually, using head movements, while keeping their body as immobile as possible. No specific indications were given with respect to the velocity, amplitude, or rate of said movements. Each participant conducted three repetitions of 3 min of visual exploration.

The natural head movements of participants were measured at 120 Hz with an IMU (XSens Dot, Movella) with the same experimental protocol described for the self-navigation task. In total, 97 min and 56 s of head velocity signals was recorded.

Data Analysis

All data analysis was performed in the Python programming language: we used the scipy package for all statistical analysis and frequency analysis.

Filtering.

In the manual navigation task, each data sample measured by the HObIT was coupled with a quality value. This quality value was determined by the number of fiducial markers in

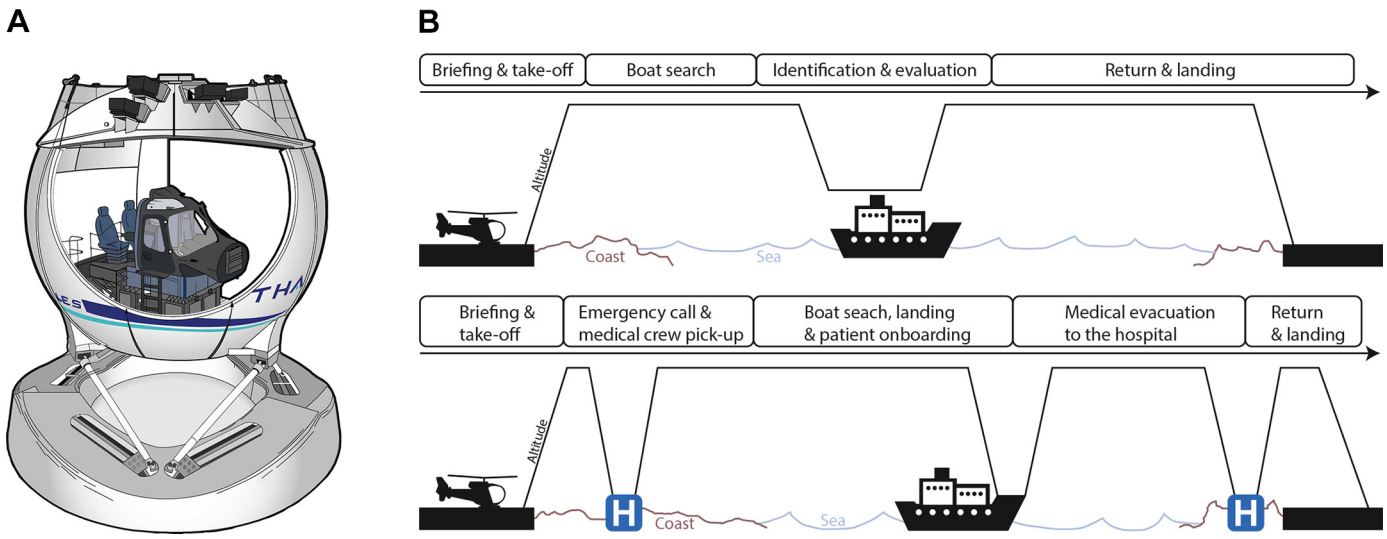

Figure 1. *A*: full flight simulator (FFS). The helicopter cabin (EC135) is located in the display dome. A 6-degrees-of-freedom motion platform drives the movements of the simulator. *B*: main tasks involved in the first (*top*) and second (*bottom*) scenarios. See Supplemental Fig. S1 for more details on the scenarios.

the field of view of the sensor. When the pilot's head was located within the optimal optical tracking zone, the quality values were maximal. When pilots moved their head away, the quality value dropped accordingly. To ensure that only reliable measurements were included in the analysis, samples associated with a quality value below a given threshold were labeled as missing values (see Supplemental Fig. S2 for more details on sample quality). This resulted in a variable yet often noticeable data loss (2.9–36.3%).

Missing values.

After the filtering step, two techniques designed to process the missing values of the manual navigation task were evaluated. The first was to discard all missing values. With the end goal of assessing the frequency content of the velocity signals in mind, such a strategy could create high-frequency artifacts due to the discontinuous nature of the signal. In an effort to mitigate this effect, we explored a second technique: an autoregressive (AR) model was used to interpolate the missing values. The interested reader may find more details on the comparison of these two approaches in Supplemental Fig. S3. Both methods led to nearly equal results in terms of frequency content. In particular, no high-frequency artifacts were observed over the frequency range of interest (see Supplemental Fig. S3C). Hence, the simpler method, i.e., the first one, was employed in the rest of the analysis.

Velocity computation.

The angular velocity of the head was obtained by numerical derivation of the head's orientation or accessed directly from the IMU's gyroscopes. The velocity signals were projected onto the planes of the semicircular canal, left anterior-right posterior (LARP), right anterior-left posterior (RALP), and yaw (YAW), according to Ref. 1, using the following rotation matrix:

$$\begin{pmatrix} v_{\mathrm{LARP}} \\ v_{\mathrm{RALP}} \\ v_{\mathrm{YAW}} \end{pmatrix} = \begin{pmatrix} \cos(\theta) & -\sin(\theta) & 0 \\ \sin(\theta) & \cos(\theta) & 0 \\ 0 & 0 & 1 \end{pmatrix} \begin{pmatrix} \cos(\gamma) & 0 & -\sin(\gamma) \\ 0 & 1 & 0 \\ \sin(\gamma) & 0 & \cos(\gamma) \end{pmatrix} \begin{pmatrix} v_x \\ v_y \\ v_z \end{pmatrix}$$

with $\theta = 45^\circ$ and $\gamma = 18^\circ$.

Probability density functions.

Probability density functions were computed with a Gaussian-kernel density estimation evaluated between -200°/s and $+200^\circ$/s with a step of 5°/s. Deviation from normality was quantified by the excess kurtosis and computed as follows:

$$K = \frac{\langle (X-\mu)^4 \rangle}{\sigma^4} - 3$$

where X represents the LARP, RALP, or YAW angular velocity signal, μ and σ its mean and standard deviation, respectively, and $\langle \cdot \rangle$ the average.

Power spectral densities.

Power spectral densities were computed as described in Ref. 3. Briefly, Welch's average periodogram was used with a length of the fast Fourier transform $nfft$ = 2,048 and a Bartlett window of n_{window} = 2,048 samples. These parameters led to a frequency resolution of ~0.05 Hz (resp. 0.06 Hz) in the manual navigation task (resp. in the self-navigation and seated visual exploration tasks) given an input sampling frequency of 100 Hz (resp. 120 Hz).

As per previous works in the literature (1–3), the power spectra obtained in the manual navigation task were fitted with two power laws. The first fit spanned the low frequencies, from 0.1 to 1 Hz. The second fit spanned the high frequencies, from 4 to 20 Hz. The boundary values were chosen such that the frequency bands they define correspond to the usual ranges found in neurophysiological studies (9, 10) while also reflecting the behavior observed in our data. For instance, compared to Carriot et al. (1), this entailed a decrease of the higher bound of the low-frequency range, from 2 Hz to 1 Hz, and of the lower bound of the high-frequency range, 4 Hz instead of 10 Hz. This shift in bounds accounts for the lower transition frequency found in our results, defined as the transition between the two regimes. The upper bound for the high-frequency range was also decreased, 20 Hz rather than 30 Hz, to avoid fitting on power values below the signal's noise level, as defined by the sensors' baseline noise power (~$0.01^{\circ 2}$/s).

In the manual navigation task, a further distinction was made between epochs of gaze-redirecting and gaze-stabilizing head movements. Using a simple classification algorithm (see *Discriminating gaze-redirecting vs. gaze-stabilizing head movements*), we partitioned the head velocity signals into a collection of short gaze redirection and gaze stabilization sequences. Their respective power spectra were then computed with the Lomb–Scargle periodogram, a particular kind of least-squares spectral analysis that estimates a frequency spectrum when data samples are not equally spaced in time (11).

Discriminating gaze-redirecting vs. gaze-stabilizing head movements.

In ecological settings, humans use a coordinated eye and head movement to shift their gaze to a new target of interest (12–20). When the head is in motion and the gaze is fixated on a target of interest, the vestibulo-ocular, the cervico-ocular, and the optokinetic reflex intervene to stabilize the image of the environment on the retina (21–23) by counterrotation of the eyes in the direction opposite to the head movement. To assess the contribution of gaze-redirecting and gaze-stabilizing head movements to the shape of the spectra in the manual navigation task, we isolated both components, using a basic classification algorithm. Head movements that occurred simultaneously with an eye movement in the same direction were considered gaze-reorienting head movements. Conversely, those that occurred with a concomitant eye movement in the opposite direction were considered gaze-stabilizing movements.

Statistical analysis.

The Mann–Whitney–Wilcoxon test was used to measure statistical similarity, or lack thereof, of the characteristics of head movements in the different planes of the semicircular canals between the different experiments. The Wilcoxon signed-rank test was used to measure statistical similarity, or lack thereof, of the characteristics of head movements in each experiment between the different planes of motion.

RESULTS

Statistics of Head Angular Velocity

The statistics of natural vestibular stimuli experienced by the participants during the manual navigation task, the self-navigation task, and the seated visual exploration task were characterized. To that end, the angular velocity of participants' head movements was projected onto the three planes of the semicircular canals to assess the corresponding vestibular inputs independently (Fig. 2*A*).

We found that the velocity distribution varied greatly across experiments (Fig. 2*B*). In all planes of motion, the interquartile range differed significantly between the self-navigation and manual navigation tasks ($P < 0.01$, Mann–Whitney–Wilcoxon test), as well as between the self-navigation and the seated visual exploration tasks ($P < 0.01$), but did not differ between the manual navigation and seated visual exploration tasks ($P > 0.05$, although we note a P value of $P \approx 0.05$ in the YAW plane). Hence, significantly smaller-velocity head movements were observed in the two seated tasks compared to self-navigation. Additionally, whereas the spread of head angular velocity showed no significant difference between the three planes of motion in the self-navigation and visual exploration tasks ($P > 0.05$ except for RALP vs. YAW during self-navigation, where $P > 0.04$), it differed significantly in all planes during the manual navigation task (LARP vs. RALP: $P < 0.01$, LARP vs. YAW: $P < 0.01$, and RALP vs. YAW: $P < 0.01$).

We computed the probability density functions of the head angular velocity signals (Fig. 2*C*). In all activities, the distributions were characterized by their non-Gaussian nature, with a sharp peak centered on zero and large tails. Deviation from normality was quantified with the excess kurtosis (Fig. 2*C*, *insets*). All distributions presented excess kurtosis values that differed significantly from zero ($P < 0.01$, Wilcoxon signed-rank test), but only the excess kurtosis values from the manual navigation task differed significantly from the others in all planes of motion ($P < 0.01$, Mann–Whitney–Wilcoxon test).

Frequency Content of Head Angular Velocity Signals

We measured the frequency content of vestibular stimuli in all experiments by computing their power spectra (Fig. 3). As previously reported, we found that the power followed a double power law in the three planes of the semicircular canals during self-navigation (Fig. 3, blue) (1–3). Quantitatively, the slopes of the fits (cf. legend of Fig. 3) were consistent with those described in Carriot et al. (1). However, we noted a pronounced decrease in the frequency value that marks the transition between the two regimes compared to the latter. The aforementioned authors found that active head movements shape the structure of vestibular stimuli. Together, these results suggest

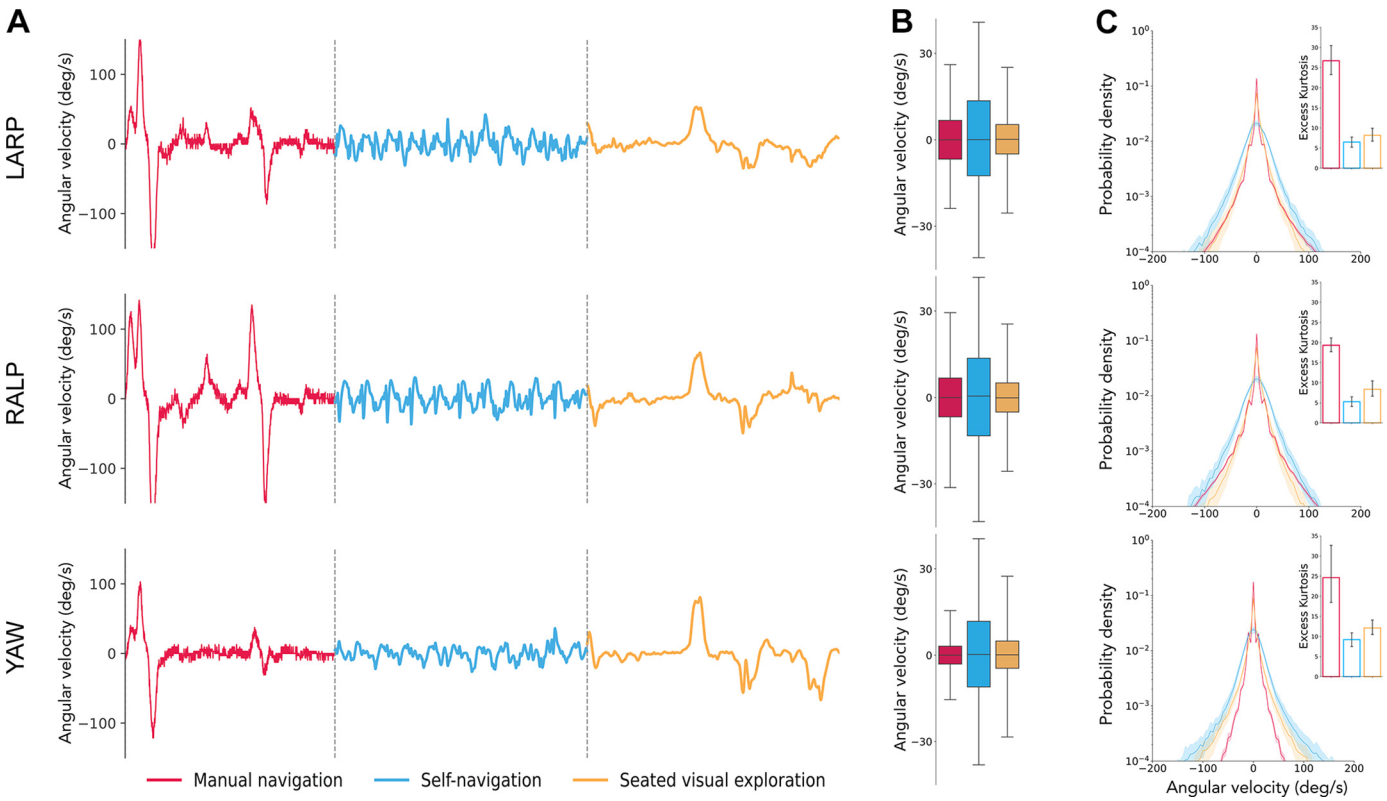

Figure 2. *A*: 10-s excerpts of the angular velocity signals in the 3 planes [left anterior, right posterior (LARP) plane, right anterior, left posterior (RALP) plane, and yaw plane (YAW)] of the semicircular canals in the manual navigation task (red), in the self-navigation task (blue), and during seated visual exploration (orange). Each signal corresponds to a single participant ($n = 1$ subject). *B*: boxplot of the population-averaged (red, $n = 7$ subjects; blue, $n = 11$ subjects; orange, $n = 11$ subjects) angular velocity signals projected in the 3 planes of the semicircular canals in the 3 experiments. Boxes and whiskers correspond to 75% and 95%, respectively, of the data. Outliers are not represented. *C*: population-averaged (red, $n = 7$ subjects; blue, $n = 11$ subjects; orange, $n = 11$ subjects) probability density functions for the LARP, RALP, and YAW head velocity signals in the manual navigation task (red), in the self-navigation task (blue), and during seated visual exploration (orange) with corresponding SD (shaded areas). *Insets*: population-averaged (red, $n = 7$ subjects; blue, $n = 11$ subjects; orange, $n = 11$ subjects) excess kurtosis values. The error bars represent the 95% confidence interval.

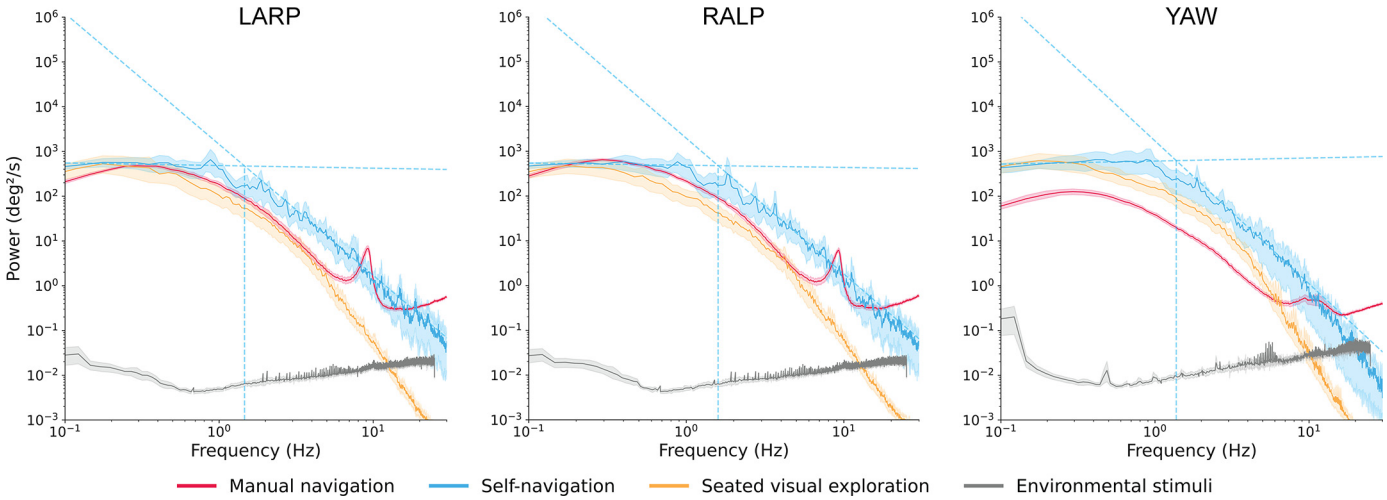

Figure 3. Population-averaged (red, $n = 7$ subjects; blue, $n = 11$ subjects; orange, $n = 11$ subjects) power spectra of the head angular velocity in the left anterior, right posterior (LARP), right anterior, left posterior (RALP), and yaw (YAW) planes with corresponding 95% confidence interval (shaded areas). Red, manual navigation task; blue, self-navigation task; orange, seated visual exploration; gray, environmental stimuli (helicopter cabin). The blue dashed lines correspond to power law fits of the power spectra. The characteristics of the fits are as follows: slope of the LARP low-frequency fit = $-0.06 \pm 0.12^{\circ 2}$, slope of the LARP high-frequency fit = $-2.92 \pm 0.08^{\circ 2}$, transition frequency = 1.46 ± 0.29 Hz; slope of the RALP low-frequency fit = $-0.05 \pm 0.08^{\circ 2}$, slope of the RALP high-frequency fit = $-3.03 \pm 0.11^{\circ 2}$, transition frequency = 1.59 ± 0.33 Hz; slope of the YAW low-frequency fit = $-0.07 \pm 0.09^{\circ 2}$, slope of the YAW high-frequency fit = $-3.19 \pm 0.11^{\circ 2}$, transition frequency = 1.37 ± 0.22 Hz.

an effect of task intensity on the transition frequency between the two fits. Indeed, the intensity required during the self-navigation task in this study was lower than that of some of the activities investigated in Carriot et al. (1), such as jumping up and down, playing soccer, etc., which could account for the observed decreased transition frequency value.

In both the manual navigation (Fig. 3, red) and seated visual exploration (Fig. 3, orange) tasks the power spectra could no longer be fitted by two power laws. In the three planes of motion, the power spectra followed an inverted "U" shape: the power increased up to a maximum at ~0.3 Hz before decreasing slowly up to 6 Hz. For frequencies above 6 Hz, we observed a clear dichotomy in the shape of the spectra between the visual exploration and manual navigation tasks. Whereas the power continued to decrease following the inverted U shape in the visual exploration experiment, some sort of peak appeared in the power spectra in the LARP and RALP planes of the manual navigation task, rapidly boosting the power up again (see DISCUSSION for more information on this matter). Furthermore, compared to the other experiments, where the general shape of the spectra is invariant in all planes of motion, the power in the YAW plane of the manual navigation task was unique. The spectra lacked a clear peak of frequency and showed a lower total average power compared with the other signals. Overall, we observed no effect of flight experience (Supplemental Fig. S4A) or scenario (Supplemental Fig. S4B) on the shape of the power spectra for the manual navigation task. Our results suggest that both seated tasks induce an unusual structure in natural vestibular stimuli.

Different Activities Led to Different Frequency Contents

We wondered how the particular shape of the power spectra measured during the seated visual exploration or manual navigation task would reflect the frequency content of vestibular inputs. In a recent paper, Sinnott, Hausamann, and MacNeilage (24) demonstrated that head reorientation movements predominated at low frequencies (≈0–1 Hz), whereas head translation movements prevailed at higher frequencies (>1 Hz). Following their work, we partitioned the frequency range into two bands to quantify the relative contribution of each band to the total power (Fig. 4). The first spanned 0–1 Hz, and the second ranged from 1 to 6 Hz. This upper limit was chosen so as to prevent misrepresentation of natural stimuli caused by artifacts in higher frequencies (e.g., the peak in the manual navigation task). This segregation also conveniently corresponds to the usual classification of head movements used in neurophysiological studies. For instance, O'Leary and Davis (9) proposed the range 2–6 Hz to define high-frequency active head movements in their work.

We found that the low-frequency band constitutes the dominant contribution to the total power of the angular velocity signals in all tasks. In the LARP and RALP planes, all contributions were significantly different ($P < 0.05$, Mann–Whitney–Wilcoxon test) and followed the same order. By descending order of contribution, we first had the seated tasks with the seated visual exploration and the manual navigation and then the self-navigation. Naturally, results are similar but reversed for the high-frequency band: contributions are all statistically significant in the LARP and RALP planes, with a greater contribution observed in the self-navigation task. We also found no statistical differences ($P > 0.05$) in the contribution of the bands to the total power between the different planes of motion. Thus, our results indicate that the different shapes of the power spectra capture activity-specific frequency contents, namely a greater contribution of the low frequencies in the seated tasks compared to self-navigation, and conversely a larger contribution of the high frequencies in the self-navigation task compared to the seated tasks.

Gaze-Redirecting vs. Gaze-Stabilizing Head Movements during Manual Navigation

We computed the power spectra of gaze-redirecting (Fig. 5, red) and gaze-stabilizing (Fig. 5, blue) head movements in the manual navigation task. The shape of the spectra for the

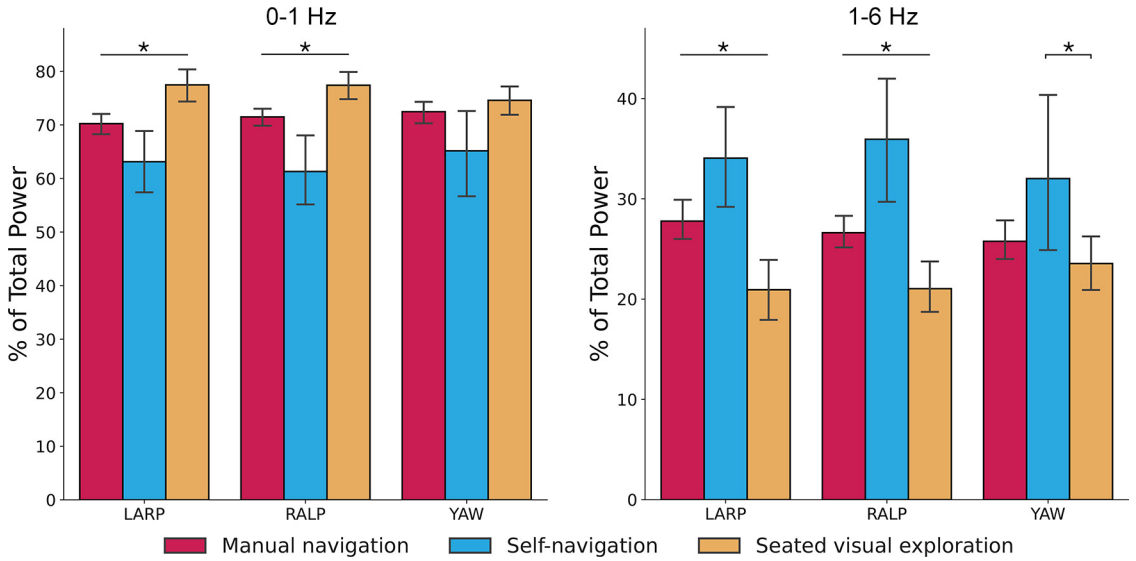

Figure 4. Contribution of the 0–1 Hz (*left*) and 1–6 Hz (*right*) frequency bands to the total spectral power, expressed as a percentage, in the 3 planes [left anterior, right posterior (LARP) plane, right anterior, left posterior (RALP) plane, and yaw plane (YAW)] of the semicircular canals during the manual navigation task (red $n = 7$ subjects), the self-navigation task (blue $n = 11$ subjects), and the seated visual exploration task (orange $n = 11$ subjects). Error bars represent the 95% confidence interval. *Statistical significance is reported for $P < 0.05$ (Mann–Whitney–Wilcoxon tests). Note the variations in the range of the *y*-axis.

stabilizing motions qualitatively resembled the results presented in Fig. 3 (red), with an inverted U shape and a peak in the LARP and RALP planes from 6 to 10 Hz. Gaze-redirecting movements also presented the characteristic U shape but with a slower falloff in the high frequencies compared to the others. These movements also did not present any peak in the power spectra relative to the power measured in the high-frequency band.

DISCUSSION

In this study, we measured and characterized the vestibular stimuli experienced by healthy participants in a variety of real-world activities. We were able to reproduce previous results during a self-navigation task and broadened the scope of research with a seated visual exploration task and an interaction with a complex human-machine interface: a helicopter simulator. Our analysis focused on the angular velocity of head movement projected onto the three planes of the semicircular canals. We derived statistical metrics from these signals and investigated their frequency content through their power spectra, according to prior works (1, 3).

We found that the velocity distribution of head movements in the two seated tasks contained significantly greater low-velocity values than during self-navigation. Interestingly, the spread of these distributions, as quantified by the interquartile range, was invariant across the LARP, RALP, and YAW planes in all activities except for the manual navigation task, where distributions varied significantly across all planes. The signals' associated probability density functions differed significantly

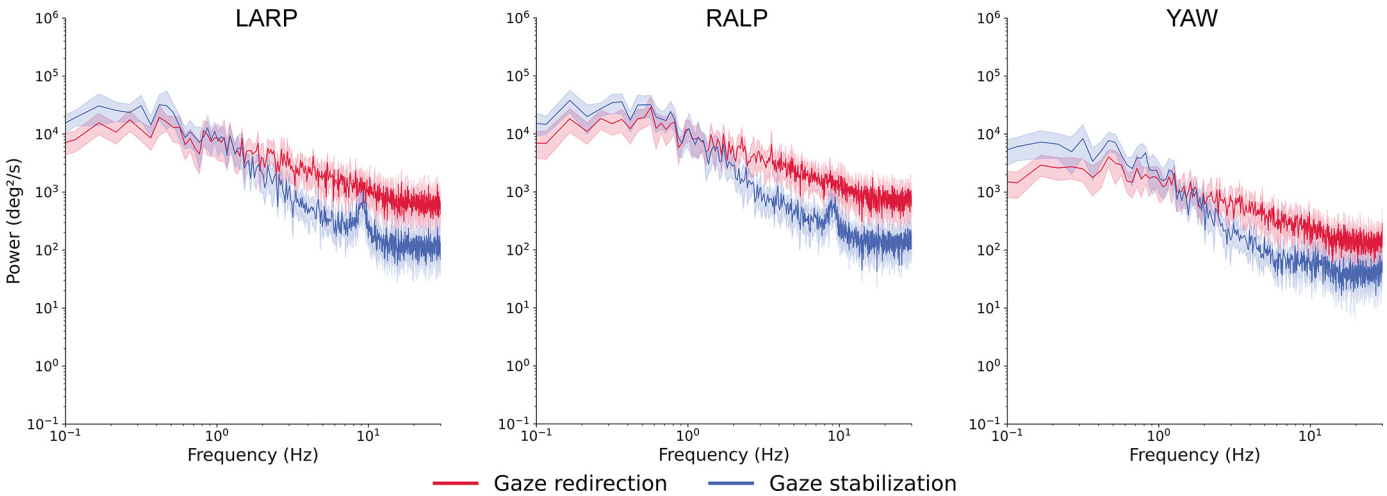

Figure 5. Population-averaged ($n = 7$ subjects) power spectra of the head angular velocity signals of participants in the manual navigation task during gaze redirection (red) and gaze stabilization (blue) epochs, with corresponding 95% confidence interval (shaded areas). These spectra were computed with the Lomb–Scargle periodogram method. LARP, left anterior, right posterior plane; RALP, right anterior, left posterior plane; YAW, yaw plane.

from normality, with a sharp peak centered on zero and long tails. In all planes of motion, excess kurtosis values differed significantly between the manual navigation task and the others.

We then showed that the frequency content of the vestibular stimuli varied across experiments. For the self-navigation task, we were able to fit the power spectra with the same two-power law model proposed in the literature (1, 3). For the other two experiments, however, the power spectra presented a surprising inverted U shape, which caused the power to fall off more rapidly in the higher frequencies (>1 Hz) than during self-navigation. This unusual shape led to a higher spectral content of low frequencies (0–1 Hz) than high frequencies compared with the self-navigation task.

Taken together, our findings suggest that *1*) natural activities such as walking provoke stereotyped vestibular inputs whose power spectra can be modeled by two power laws that intersect at a task intensity-dependent frequency; *2*) body posture induces changes in the frequency content affecting the vestibular organs; *3*) pilots tend to operate their machines in a way that does not generate highly nonecological vestibular stimuli; and *4*) nevertheless, human-machine interfaces used as a means of manual navigation impose some unnatural, contextual constraints on their operators.

Head movement velocity distributions differed significantly between seated and standing experiments in all planes of motion. When seated, whether in the manual navigation or the seated visual exploration task, the spread of the distributions of head angular velocity was smaller than when walking. Could this apparent restriction in the spectrum of possible head motion velocity originate from a physiological limitation imposed by the seated condition? Indeed, in daily activities, humans reorient their visual axis using a combination of eye, head, trunk, and foot movements (25, 26). This intersegmental coordination can lead to greater head velocity, as it is the sum of head-on-neck velocity, trunk-on-pelvis velocity, and foot-on-ground velocity. On the contrary, when seated, only the neck, and eventually the trunk, contributes to the total head rotation. Yet, in our experiments the limited freedom of body movement did not seem to impair the possible range of head velocity, as they routinely reached values similar to those measured during self-navigation. Said differently, task- and context-dependent adaptations rather than physiological constraints shape the range of head angular velocity in natural activities.

Although we found no significant difference in the range of head velocity between the manual navigation and seated visual exploration tasks, a closer look at the probability density functions of these signals reveals that there exists a significant difference in excess kurtosis between the two and no significant difference between self-navigation and seated visual exploration. This reflects the presence of a majority of low-velocity head movements and a lower but nonnegligible amount of higher-velocity head movements when piloting than during ecological activities. Pilots spend a considerable amount of time monitoring their instruments, and the low-velocity head movements measured could correspond to small-amplitude gaze shifts between panels on their interface. Because the flight instruments are predominantly stacked vertically in front of the pilot, the coupled eye and head movements tend to have a smaller horizontal component, which is consistent with the significantly smaller velocity range observed in the YAW plane compared with the others. Thus, the context of the human-machine interaction appears to impose head motions whose velocity differs from those experienced in ecological conditions. These movements are characterized by their low velocity and an asymmetry between the YAW plane and the LARP and RALP planes.

The biomechanical properties of the body act as a filter that alters the spectral content of the mechanical stimuli experienced during natural tasks (27–31). Contrary to what happens in other sensory modalities, biomechanical filtering causes the power spectra of head movements to deviate from a single power law during active and passive head movements (1–3). In this study, the seated visual exploration task only consisted of active head movements, with neither self-induced mechanical perturbations (the subjects were sitting still) nor environmental stimuli or vibrations (the chair was stationary), yet the shape of the power spectra still deviated from a single power law. Hence, sitting imposed a set of anatomical and physiological constraints that altered the frequency content of natural vestibular stimulation in a different way than during standing activities. In other words, we propose that different skeletal configurations modify the characteristics of natural head motion, acting as some sort of "anatomical" filter that combines with the more passive biomechanical filter mentioned above. In support of that view, our results during the self-navigation task are in good accordance with those of prior studies (1–3), i.e., when subjects were in a standing position. On the other hand, they differ from previous work in seated subjects, most probably because in these studies the subjects wore a neck brace that suppressed head-on-body motion.

Whereas the overall shape of the power spectra of head angular velocity was similar in both of the seated tasks investigated, the manual navigation task presented an additional peak in the range 6–10 Hz that was not present in the seated visual exploration task. Because of its relatively high frequency, we found it unlikely that it was caused by voluntary physiological movements. We considered two plausible sources for this peak: *1*) a measurement artifact affecting the sensor or *2*) the presence of vibrational perturbations in the immediate environment of the pilot. Additional tests performed on the head tracking sensor (not shown here) proved its reliability and robustness against potential electromagnetic pollution from neighboring sensors, which would tend to rule out *hypothesis 1*, but revealed its sensitivity to mechanical perturbations. To be more specific, the head-mounted HObIT was placed at the end of a stiff but flexible metal rod, the extremity of which could vibrate in the 6–12 Hz frequency range when subjected to external disturbances. Comparing the estimations of the power spectra during gaze-redirecting (Fig. 5, red) and gaze-stabilizing (Fig. 5, blue) head movements, we found that only the latter presented a peak relatively to the power measured. In brief, the aforementioned vibration might still exist in gaze-orienting motions but is dominated by the frequency content of the voluntary head movement: as previous works have established, active head movements shape the structure of natural vestibular stimuli (1). The presence of this 6–10 Hz peak in the spectra of head velocity during gaze-stabilizing movements directly suggests that only a partial stabilization of the head is achieved in

response to exogeneous perturbations, which are common in a helicopter cabin (see Fig. 3, black and Supplemental Fig. S5). It is therefore possible that pilots were subjected to relatively high-frequency vibrations, unfortunately not quantifiable given the experimental apparatus, that they cannot fully compensate for. Hinz et al. (32) demonstrated that seat-to-head vibration transmissibility curves presented a peak around 8 Hz when using a backrest. Accordingly, we postulate that the peak in the power spectra was caused during reflexive passive head movements in response to perturbations generated by the movement of the cabin and transmitted to the head via the seat. Such vibrations could, in the long run, induce musculoskeletal disorders in the operators (33): multiple studies have evaluated the effect of whole body vibrations (WBVs) and found that occupations with high exposure to WBV are at risk for the development of pathologies of the neck and shoulder complex (32, 34).

It is commonly assumed that, during active behavior, the expected sensory information produced by body movements is compared to the actual sensory information experienced to finely tune motor control (35, 36). Using *efference copies* of motor commands, humans are able to distinguish between self-generated and externally applied movements. Evidence for this mechanism was put forward by extracellular single-unit measurements of the vestibular nuclei in primates. For instance, Cullen and Roy (35) reported that the neuronal response to self-generated head movements was greatly attenuated in the vestibular nuclei during active head-on-body motion (e.g., 70% during gaze shifts). In pilots, vestibular information stems from an overlap of two sources: their voluntary head movements, of course, but also the vehicle-induced vestibular inputs caused by their actions on the commands or caused by external perturbations. Roy and Cullen (37) showed in rhesus monkeys that vestibular-only (VO) neurons, the neurons that are thought to mediate at least partly the vestibulo-collic reflex (VCR) pathway, reliably encoded passive head rotations, even when they co-occurred during active head movements and even when the passive head movements were self-induced (e.g., when passive whole body rotations were self-generated with a steering wheel). Thus, prior works suggest a differential processing of vestibular information (at the level of the vestibular nuclei) based on whether the movement was actively generated by the individual or was passively experienced. We believe that pilots are ideal candidates to study the selective processing of passively applied vestibular inputs. In particular, we may wonder whether the pilots have developed, perhaps through experience, an appreciation of the relationship that binds the movements they impose on the commands to the movements of their head in space. Can pilots effectively predict the sensory consequences of their action on the manipulanda, or do they rely on an iterative sampling of instantaneous sensory information? In other words, can passive yet self-induced movements of the head be predicted when using complex machines? That is, can humans produce an efferent copy that integrates the characteristics of the machines they operate and compare it with the reafferent sensory inputs that result from their goal-directed action on the manipulanda? The present results tend to imply that the pilots were able to do so to some extent. Indeed, the qualitative similarity between the vestibular inputs experienced in the seated visual exploration task and the manual navigation task points to some level of prediction of the aircraft's dynamics. This raises the question of whether these potential predictive capabilities are the product of a thorough understanding of the machine's finer characteristics or a self-limitation of its capabilities within an operating range that approximates ecological conditions. Such issues remain to be explored; we propose to examine them in greater details through the prism of *embodiment* (38–40).

Limitations

Because of difficulties with pilot availability, it was not possible for the pilots to perform the self-navigation and the seated visual exploration experiments. The subjects who conducted the self-navigation and seated visual exploration tasks matched, however. Although it is undoubtedly a major limitation of the present study that the same subjects were not tested under all conditions, care was taken to constitute a similar, age-matched group to support the comparison. Hence, we made the implicit assumption that the characteristics of head movements in healthy individuals are sufficiently stereotyped to be comparable.

In addition, the experimental equipment used in the manual navigation task was unable to assess the natural vestibular inputs caused by linear accelerations along the fore-aft, interaural, and vertical directions, which is unfortunate as linear motion has been studied in prior studies of ecological vestibular statistics.

Furthermore, the surge in frequency in the range 6–10 Hz of the power spectra, indicative of the existence of mechanical disturbances in the immediate environment of the pilots, did not allow us to precisely quantify the contribution of high-frequency vestibular inputs during piloting. Future experiments should conceive a new head-tracking measurement system suitable for the context of complex human-machine interfaces.

We did not find any effect of pilot experience on the statistics of head movements. However, the concept of experience in this study was difficult to assess (Number of hours spent in a real helicopter? In a simulator? Over the whole career? In the last few months?). Nonetheless, the sample size may have been too small to draw any firm conclusions.

The second scenario in the manual navigation task was designed to be more challenging. Although we expected to observe more dynamic simulator movement and therefore different head movement statistics, we did not find significantly different results between the two scenarios. This may indicate that, despite the difficulty of the task, pilots are committed to controlling the helicopter so that its motion does not generate sensory inputs that are too different from what they usually experience. We believe that perturbation protocols are well suited to investigate this issue further, i.e., to assess head movement characteristics in response to ecological turbulence (bad weather conditions, etc.) or nonecological perturbations (impulse noise in simulator motion, etc.), and plan to do so in a subsequent study.

Conclusions

As human-machine interfaces become increasingly central to our everyday lives, it is important to understand how

their use may affect our sensory inputs. By measuring the angular velocity of the head during three different tasks, this study established a significant impact of body posture, notably sitting versus standing up, on the statistics and frequency content of vestibular stimuli, revealing that the physiological constraints imposed by activity-specific skeletal configurations shape vestibular inputs. During active head movements in standing activities, our results also suggest an effect of task intensity on the transition frequency between the low- and high-frequency regimes in the power spectra. Although subjected to rather unecological vestibular stimuli caused by the helicopter's motion, the pilots produced head movements whose characteristics were reminiscent of those observed in a natural task while seated. The specific processing of passive, self-induced head movement appears to be an essential mechanism to assess in the operators of complex machines. In particular, it could shed light on whether, and if so to what extent, the characteristics of the machine can be integrated into the pilot's internal forward model.

DATA AVAILABILITY

Data will be made available upon reasonable request.

SUPPLEMENTAL MATERIAL

Supplemental Figs. S1–S5: https://doi.org/10.5281/zenodo.8016675.

ACKNOWLEDGMENTS

The authors are grateful for the work of Thales engineers who made the simulator experiments possible. The authors also express heartfelt appreciation to the two anonymous reviewers for insightful feedback and guidance.

GRANTS

This work was funded by CIFRE grant No. 2022/0467 from the Association Nationale de la Recherche et de la Technologie (ANRT) awarded to A. Roques. This work was also supported by the Quantico industrial chair.

DISCLAIMERS

The funders had no role in study design, data collection and analysis, decision to publish, or preparation of the manuscript.

DISCLOSURES

No conflicts of interest, financial or otherwise, are declared by the authors.

AUTHOR CONTRIBUTIONS

A.R., Y.J., and P.-P.V. conceived and designed research; A.R. and Y.J. performed experiments; A.R. analyzed data; A.R., Y.J., and P.-P.V. interpreted results of experiments; A.R. prepared figures; A.R. drafted manuscript; A.R., Y.J., I.B., D.K.S., and P.-P.V. edited and revised manuscript; A.R., Y.J., I.B., D.K.S., N.V., and P.-P.V. approved final version of manuscript.

REFERENCES

1. **Carriot J**, **Jamali M**, **Chacron MJ**, **Cullen KE.** Statistics of the vestibular input experienced during natural self-motion: implications for neural processing. *J Neurosci* 34: 8347–8357, 2014. doi:10.1523/JNEUROSCI.0692-14.2014.
2. **Carriot J**, **Jamali M**, **Cullen KE**, **Chacron MJ.** Envelope statistics of self-motion signals experienced by human subjects during everyday activities: implications for vestibular processing. *PLoS One* 12: e0178664, 2017. doi:10.1371/journal.pone.0178664.
3. **Zobeiri OA**, **Ostrander B**, **Roat J**, **Agrawal Y**, **Cullen KE.** Loss of peripheral vestibular input alters the statistics of head movement experienced during natural self-motion. *J Physiol* 599: 2239–2254, 2021. doi:10.1113/JP281183.
4. **Wark B**, **Lundstrom BN**, **Fairhall A.** Sensory adaptation. *Curr Opin Neurobiol* 17: 423–429, 2007. doi:10.1016/j.conb.2007.07.001.
5. **Kingstone A**, **Smilek D**, **Ristic J**, **Kelland Friesen C**, **Eastwood JD.** Attention, researchers! It is time to take a look at the real world. *Curr Dir Psychol Sci* 12: 176–180, 2003. doi:10.1111/1467-8721.01255.
6. **Kingstone A**, **Smilek D**, **Eastwood JD.** Cognitive ethology: a new approach for studying human cognition. *Br J Psychol* 99: 317–340, 2008. doi:10.1348/000712607X251243.
7. **Golding JF**, **Gresty MA.** Biodynamic hypothesis for the frequency tuning of motion sickness. *Aerosp Med Hum Perform* 87: 65–68, 2016. doi:10.3357/AMHP.4295.2016.
8. **Cullen KE.** Vestibular processing during natural self-motion: implications for perception and action. *Nat Rev Neurosci* 20: 346–363, 2019. doi:10.1038/s41583-019-0153-1.
9. **O'Leary DP**, **Davis LL.** High-frequency autorotational testing of the vestibulo-ocular reflex. *Neurol Clin* 8: 297–312, 1990. doi:10.1016/S0733-8619(18)30357-8.
10. **Massot C**, **Schneider AD**, **Chacron MJ**, **Cullen KE.** The vestibular system implements a linear-nonlinear transformation in order to encode self-motion. *PLoS Biol* 10: e1001365, 2012. doi:10.1371/journal.pbio.1001365.
11. **VanderPlas JT.** Understanding the Lomb–Scargle periodogram. *Astrophys J Suppl* 236: 16, 2018. doi:10.3847/1538-4365/aab766.
12. **Zangemeister WH**, **Stark L.** Active head rotations and eye-head coordination. *Ann NY Acad Sci* 374: 540–559, 1981. doi:10.1111/j.1749-6632.1981.tb30899.x.
13. **Zangemeister WH**, **Stark L.** Types of gaze movement: variable interactions of eye and head movements. *Exp Neurol* 77: 563–577, 1982. doi:10.1016/0014-4886(82)90228-X.
14. **Afanador AJ**, **Aitsebaomo P**, **Gertsman DR.** Eye and head contribution to gaze at near through multifocals: the usable field of view. *Am J Optom Physiol Opt* 63: 187–192, 1986. doi:10.1097/00006324-198603000-00004.
15. **Guitton D.** Control of eye-head coordination during orienting gaze shifts. *Trends Neurosci* 15: 174–179, 1992. doi:10.1016/0166-2236(92)90169-9.
16. **Fuller JH.** Head movement propensity. *Exp Brain Res* 92: 152–164, 1992. doi:10.1007/BF00230391.
17. **Stahl JS.** Amplitude of human head movements associated with horizontal saccades. *Exp Brain Res* 126: 41–54, 1999. doi:10.1007/s002210050715.
18. **Einhäuser W**, **Schumann F**, **Bardins S**, **Bartl K**, **Böning G**, **Schneider E**, **König P.** Human eye-head co-ordination in natural exploration. *Network* 18: 267–297, 2007. doi:10.1080/09548980701671094.
19. **Pelz J**, **Hayhoe M**, **Loeber R.** The coordination of eye, head, and hand movements in a natural task. *Exp Brain Res* 139: 266–277, 2001. doi:10.1007/s002210100745.
20. **Thumser ZC**, **Oommen BS**, **Kofman IS**, **Stahl JS.** Idiosyncratic variations in eye-head coupling observed in the laboratory also manifest during spontaneous behavior in a natural setting. *Exp Brain Res* 191: 419–434, 2008. doi:10.1007/s00221-008-1534-2.
21. **Robinson DA.** The oculomotor control system: a review. *Proc IEEE* 56: 1032–1049, 1968. doi:10.1109/PROC.1968.6455.
22. **Freedman EG.** Coordination of the eyes and head during visual orienting. *Exp Brain Res* 190: 369–387, 2008. doi:10.1007/s00221-008-1504-8.

23. **Klein C, Ettinger U** (Editors). *Eye Movement Research: An Introduction to Its Scientific Foundations and Applications*. Cham, Switzerland: Springer International Publishing, 2019.
24. **Sinnott C**, **Hausamann P**, **MacNeilage PR.** Natural statistics of human head orientation constrain models of vestibular processing. *Sci Rep* 13: 5882, 2023. doi:10.1038/s41598-023-32794-z.
25. **Land MF.** The coordination of rotations of the eyes, head and trunk in saccadic turns produced in natural situations. *Exp Brain Res* 159: 151–160, 2004. doi:10.1007/s00221-004-1951-9.
26. **Anastasopoulos D**, **Ziavra N**, **Hollands M**, **Bronstein A.** Gaze displacement and inter-segmental coordination during large whole body voluntary rotations. *Exp Brain Res* 193: 323–336, 2009. doi:10.1007/s00221-008-1627-y.
27. **Nigg BM**, **Liu W.** The effect of muscle stiffness and damping on simulated impact force peaks during running. *J Biomech* 32: 849–856, 1999. doi:10.1016/S0021-9290(99)00048-2.
28. **Wakeling JM**, **Liphardt AM**, **Nigg BM.** Muscle activity reduces soft-tissue resonance at heel-strike during walking. *J Biomech* 36: 1761–1769, 2003. doi:10.1016/S0021-9290(03)00216-1.
29. **Wakeling JM**, **Nigg BM**, **Rozitis AI.** Muscle activity damps the soft tissue resonance that occurs in response to pulsed and continuous vibrations. *J Appl Physiol (1985)* 93: 1093–1103, 2002. doi:10.1152/japplphysiol.00142.2002.
30. **Behling AV**, **Giandolini M**, **von Tscharner V**, **Nigg BM.** Soft-tissue vibration and damping response to footwear changes across a wide range of anthropometrics in running. *PLoS One* 16: e0256296, 2021. doi:10.1371/journal.pone.0256296.
31. **Rigoni I**, **Bonci T**, **Bifulco P**, **Fratini A.** Characterisation of the transient mechanical response and the electromyographical activation of lower leg muscles in whole body vibration training. *Sci Rep* 12: 6232, 2022. doi:10.1038/s41598-022-10137-8.
32. **Hinz B**, **Menzel G**, **Blüthner R**, **Seidel H.** Seat-to-head transfer function of seated men-determination with single and three axis excitations at different magnitudes. *Ind Health* 48: 565–583, 2010. doi:10.2486/indhealth.MSWBVI-03.
33. **Forbes PA**, **Kwan A**, **Rasman BG**, **Mitchell DE**, **Cullen KE**, **Blouin JS.** Neural mechanisms underlying high-frequency vestibulocollic reflexes in humans and monkeys. *J Neurosci* 40: 1874–1887, 2020. doi:10.1523/JNEUROSCI.1463-19.2020.
34. **Rehn B**, **Bergdahl IA**, **Ahlgren C**, **From C**, **Järvholm B**, **Lundström R**, **Nilsson T**, **Sundelin G.** Musculoskeletal symptoms among drivers of all-terrain vehicles. *J Sound Vib* 253: 21–29, 2002. doi:10.1006/jsvi.2001.4247.
35. **Cullen KE**, **Roy JE.** Signal processing in the vestibular system during active versus passive head movements. *J Neurophysiol* 91: 1919–1933, 2004 [Erratum in *J Neurophysiol* 93: 1820, 2005]. doi:10.1152/jn.00988.2003.
36. **Cullen KE.** The vestibular system: multimodal integration and encoding of self-motion for motor control. *Trends Neurosci* 35: 185–196, 2012. doi:10.1016/j.tins.2011.12.001.
37. **Roy JE**, **Cullen KE.** Selective processing of vestibular reafference during self-generated head motion. *J Neurosci* 21: 2131–2142, 2001. doi:10.1523/JNEUROSCI.21-06-02131.2001.
38. **Kiverstein J.** The meaning of embodiment. *Top Cogn Sci* 4: 740–758, 2012. doi:10.1111/j.1756-8765.2012.01219.x.
39. **Weser V**, **Proffitt DR.** Tool embodiment: the tool's output must match the user's input. *Front Hum Neurosci* 12: 537, 2018. doi:10.3389/fnins.2018.00537.
40. **Osiurak F**, **Federico G.** Four ways of (mis-)conceiving embodiment in tool use. *Synthese* 199: 3853–3879, 2021. doi:10.1007/s11229-020-02960-1.